ACS OMEGA

Open Access

http://pubs.acs.org/journal/acsodf

Article

Paper Scintillator Incorporated with Scintillator−Silica Fine Powders: Photophysical Characterization and Proof of Concept Demonstration of Tritium Detection

Hirokazu Miyoshi,* Mami Nakamura, Elizabeth M. Tsekrekas, and Luiz G. Jacobsohn*

Cite This: https://doi.org/10.1021/acsomega.4c01901

Read Online

ACCESS | Metrics & More | Article Recommendations

ABSTRACT: In order to decrease the generation of radioactive waste, it is of interest to develop a scintillator capable of absorbing tritiated solutions for efficient detection of low-energy β-particles from tritium. In this work, paper scintillator incorporated with scintillator−silica fine powders (FPs), which is composed of scintillator−silica nanoparticles (NPs) attached to silica FP, was fabricated and evaluated. The scintillator−silica NPs contained liquid scintillators benzoic acid, 2,5-diphenyloxazole (PPO), and 1,4-bis(5-phenyloxazol-2-yl) benzene (POPOP). Photophysical characterization was executed by means of photoluminescence, fluorescence lifetime, quantum efficiency, and radioluminescence under X-ray excitation. POPOP emission was confirmed by absorbing the emissions from benzoic acid and PPO. Radioluminescence results confirmed POPOP emission. Fluorescence lifetime analysis yielded a 1.29 ± 0.01 ns main fast decay (64.2%) combined with a 4.00 ± 0.04 ns slower decay (35.8%). The combined luminescence results suggested that most POPOP in the paper scintillator was solvated. At 301 nm, the average quantum efficiency from both faces of the paper scintillator was about 4%, and at 370 nm, it was about 11%. The paper scintillator detected ^{3}H β-particles by dipping the paper scintillator into tritiated water without a liquid scintillator. The counting efficiency depended on water content in the paper scintillator, and it increased to above 10% for tritium activity less than 200 dpm since it was preferentially adsorbed by vapor pressure isotopic effect and isotopic exchanged tritium on the surface of the scintillator−silica FP in the paper scintillator.

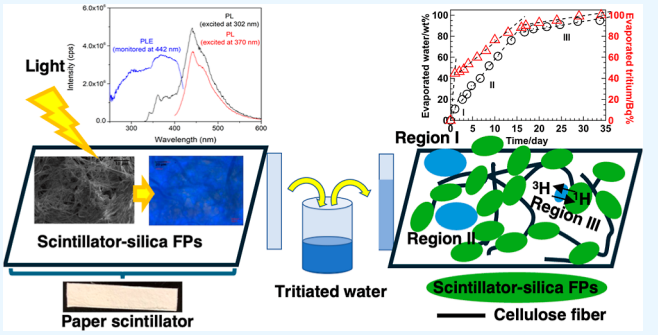

INTRODUCTION

A scintillator is a phosphor used for the detection of ionizing radiation such as X-rays, α-particles, β-particles, and γ-rays.[1,2] The radiation energy is converted to light by the scintillator, and the generated light is detected and converted to electric signal by a photodetector. A common procedure to detect β-particles is to mix a β-emitter and a liquid scintillator (LS). An LS is composed of two or three organic scintillators, for example, 2,5-diphenyloxazole (PPO) and 1,4-bis(5-phenyloxazol-2-yl) benzene (POPOP) as a wavelength shifter dissolved in organic solvents such as benzene, xylene, and toluene.[3] After the measurement of β-particles, some radioactive waste containing organic solvents is generated. Because the LS containing the β-emitter is used in a glass or a polyethylene vial, the radioactive organic solvents must be removed from the vial before it is disposed. In practice, this means the vial must be washed several times with ethyl alcohol to remove the liquid from the glass or poly vial. Therefore, a large volume of radioactive organic liquid waste is generated, typically about three times the LS original volume. In order to decrease the generation of radioactive waste, it is of interest to develop a scintillator capable of absorbing tritiated solutions for efficient detection of low-energy β-particles from tritium.

In facilities dealing with radioisotopes, a wipe test must be carried out in each experimental room every month to check for radioactive contaminants.[4] After the wipe test is completed, the wipe paper is placed in a glass or poly vial and some LS is poured into it to facilitate scintillation light generation by β-particles from a possible radioactive contaminant. A liquid scintillation counter (LSC) is used to measure the light emission from the LS excited by the β-particles. As described above, a large amount of radioactive organic liquid waste is generated. For this reason, a plastic scintillator (PS) formed without using organic solvents has been developed by Saint-Gobain Co. Ltd. However, water remains on the surface of the

Received: February 27, 2024
Revised: June 14, 2024
Accepted: June 20, 2024

PS because the PS is usually hydrophobic and does not absorb water.

Furuta and co-workers reported that atmospheric plasma treatment of the surface of a PS increased the surface contact area with water[5−8] and that water was uniformly spread on the surface over a large area of the PS. The detection efficiency of tritiated water (20 μL) having activity from 0.170 kBqL^{-1} to 80 kBqL^{-1} increased from 3.4 to 19.5% for 1 plasma-treated sheet of the PS. A set of 2 sheets achieved 47.8% compared to an efficiency of 46.6% for LS.[7] Plasma treatment of PS helped the wettability of the surface but not the absorption of water. Consequently, only the fraction of tritium emissions directed toward the scintillator can potentially be detected, with the remaining emissions being lost in air. Also, evaluation of an ultrathin or thin-film PS having a thickness of 5−100 μm to detect α- and β-particles has been reported by Morishita et al.[9] and Koshimidzu et al.[10] In fact, since β-particles from tritium have a low energy of 18.6 keV and their range is only 6 mm in air and 6 μm in water;[11] only a small fraction of all tritium emissions is actually detected by the PS. Therefore, it will be helpful to find a way to have all β-particles being emitted from inside the scintillator toward achieving efficient tritium detection.

The use of nanoparticle (NP) and nanocomposite scintillators for the detection of ionizing radiation has been proposed,[12−14] and these concepts were evoked to help the detection of tritium. Miyoshi and co-workers reported the encapsulation of the organic scintillators PPO, POPOP, and benzoic acid in silica nanoparticles.[15] Benzoic acid was selected since the excitation of benzene rings by β-particles is similar to the excitation of an organic solvent in an LS. Once the scintillator−silica NPs were in contact with tritiated water, the hydrophilic silica surface readily absorbed water into the scintillator−silica NPs. However, the size of the scintillator−silica NPs of about 9 nm[16] was too small to store tritiated water and, consequently, the counting efficiency was low. On the other hand, Janczak et al. prepared polystyrene-core, silica-shell scintillator nanoparticles (brand name "nanoSCINT") whose size was about 300 nm, and 296 Bq/ml of tritiated water was detected using 1 mg/mL of nanoSCINT suspended in aqueous solutions.[17] However, the count rate was too low compared to the background one. Therefore, a micrometer-sized silica fine powder (FP) was introduced as a platform to retain tritiated water near the scintillator−silica NPs. That is, scintillator−silica NPs were fixed on the surface of the micrometer-size silica platform, and this system was named scintillator−silica FPs.[16] The tritiated water retained by the platform effectively emitted β-particles to the nearby scintillator−silica NPs. However, because it was in powder form, this material was not easy to use. Therefore, a pellet (diameter: 13 mm; thickness: 0.6 mm) was fabricated. It was shown that a droplet of tritiated water with volume from 1 to 100 μL could pass through the surface of the pellet and be absorbed. For example, 2.4 kBq of tritium in 1, 10, and 100 μL aqueous solutions was detected using an LSC without LS, and the count rate increased with the radioactivity concentration.[18] However, the pellet could not absorb more than 100 μL of the aqueous solution because of its limited volume. Therefore, a novel material architecture was conceived. If a paper composed of scintillator−silica FPs can be made, it is likely to be able to absorb larger volumes of radioactive aqueous solutions in cellulose fibers that have significant hydrogen bond networks[19] and thus to have a wide range of applications. For example, the paper scintillator can be used to wipe a solid radioactive contaminant as well as a paper to dip into tritiated water similarly as a pH paper is used to check the pH of a solution. A major advantage is that the paper scintillator does not require LS to work and consequently generates considerably less waste. Previously, Miyoshi and Nakamura[20] reported on the fabrication of paper scintillators and their effective use in radiation testing for α- and β-particles in radioactive liquid, solid, and gas contaminants. However, that previous work did not include the photophysical characterization of the paper scintillator and did not discuss the mechanism or the effects of evaporation on the detection and counting efficiency of tritium in tritiated water. In this work, scintillator−silica FPs were used to make a paper scintillator. The photophysical characterization of the paper scintillator was evaluated by radioluminescence, photoluminescence, fluorescence lifetime, and quantum efficiency measurements toward gaining insight into its response to ionizing radiation. We also characterized the structure of the paper scintillator as well as its tritiated solution absorption and β-particle radiation detection properties.

EXPERIMENTAL PROCEDURES

Reagents. Ethyl alcohol, dimethyl sulfoxide (DMSO), tetraethyl orthosilicate (TEOS), concentrated ammonia solution (conc. NH_4OH), and benzoic acid were purchased from Wako Pure Chemicals Co. Ltd., while sodium silicate solution, 2,5-diphenyloxazole (PPO), and 1,4-bis(5-phenyl-oxazol-2-yl) benzene (POPOP) were purchased from Sigma-Aldrich Co. Ltd. All of the compounds were used without further purification. Silica FPs with a particle size of about 6.78 μm were provided by Hiroura Co. Ltd. Distilled water from a Barnstead EASYPURE RODI purification system was used for all experiments.

Preparation of the Paper Scintillator. Scintillator−silica FPs were prepared following a previously reported method.[16] The surface of 6.78 μm silica FP (1.2 g) was activated by adding 25 mL of 0.5 wt % sodium silicate solution. About 0.53 g of POPOP, 4.6 g of PPO, and 5.1 g of benzoic acid were added to a mixture of 240 mL of DMSO, 140 mL of ethyl alcohol, 10 mL of TEOS, and 75 mL of water, and then 10 mL of a concentrated NH_4OH solution was added to the mixture. Scintillator−silica FP was obtained by stirring the final solution on a hot plate at about 80 °C for 3 days.

In order to make the paper scintillator, the scintillator−silica FPs were washed with distilled water three times using a 0.1 μm membrane filter to remove sulfur byproducts. The powders were dried in a beaker at 80 °C for 1 day. Furthermore, the scintillator−silica FPs were sieved to less than 100 μm particles using a 100 μm sifter.

The paper scintillator was prepared using the scintillator−silica FPs with particle size less than 100 μm and a cellulose fiber dispersion by a proprietary paper-making method at AwaPaper Mfg., Co. Ltd. Thirty ×30 cm^2 paper scintillator sheets were obtained with a content of scintillator−silica FPs of about 160 g/m^2. Both scanning electron microscopy (SEM) and optical microscopy obtained under 365 nm LED illumination revealed, in addition to fibers with various thickness, the scintillator−silica FPs and significant porosity that allow for aqueous solution absorption. Optical microscopy was performed using a Carton microscope model NDL equipped with a CMOS camera (Engineer SL-62) and the "Measure" software. SEM was performed using a JEOL JSM-6510 scanning electron microscope.

https://doi.org/10.1021/acsomega.4c01901
ACS Omega XXXX, XXX, XXX−XXX

Photophysical Characterization. Photoluminescence emission and excitation measurements were executed by using an Edinburgh Instruments FLS-1000 spectrofluorometer equipped with a 450 W Xe lamp and dual monochromators for both emission and excitation. Excitation and emission spectra were obtained with the bandwidth fixed at 0.1 nm. The number of detected photons was automatically corrected by the instrument's software for the background and spectral differences in excitation intensity and detection sensitivity.

The absolute fluorescence quantum efficiency was determined using a 120 mm diameter Edinburgh Instruments N-M01 integrating sphere coated with $BaSO_4$ coupled to an Edinburgh Instruments FLS-1000 spectrofluorometer. Excitation was set at 301 nm (bandwidth = 9 nm) and at 370 nm (bandwidth = 4.3 nm). Excitation was integrated within 290−315 and 358−380 nm, respectively, to determine the number of excitation photons. Emission was integrated within the 415−700 and 380−700 nm ranges for the 301 and 370 nm excitations, respectively. Both sides of a ca. 1 × 1 cm^2 sheet were measured under these conditions, and the average quantum efficiency value is reported.

Fluorescence lifetime measurements were executed with an Edinburgh Instruments FLS-1000 spectrofluorometer using picosecond pulsed LEDs EPLED-365 emitting at 362.8 nm (11.8 nm fwhm bandwidth, 884.0 ps pulse width at 10 MHz). A 4 nm bandwidth was used for detection with the monitoring wavelength being set at 442 nm, while the EPLED repetition rate was fixed at 5 MHz. The instrumental response function (IRF) was determined under identical conditions, but with the EPLED light being reflected by the sample into the detector and detection set at 362.8 nm. Numerical reconvolution to remove broadening effects due to instrumental resolution and best fitting using two exponential decays were executed to extract lifetime values and relative contributions using FAST 6.0 software and the experimentally determined IRF.

Radioluminescence measurements were executed using a customer-designed configuration of the Freiberg Instruments Lexsyg Research spectrofluorometer equipped with a Varian Medical Systems VF-50J X-ray tube with a tungsten target. The X-ray source was coupled to an ionization chamber for continuous irradiation intensity monitoring. The light emitted by the sample was collected into an Andor Technology SR-OPT-8024 optical fiber connected to an Andor Technology Shamrock 163 spectrograph coupled to a cooled (−80 °C) Andor Technology DU920P-BU Newton CCD camera (spectral resolution was ca. 0.5 nm/pixel). RL measurements were executed under continuous X-ray irradiation (40 kV, 1 mA) at room temperature.

Detection of Tritium by the Dipping Paper Scintillator into Tritiated Water. Five × 1 cm^2 strips of paper scintillator (101.4 ± 0.6 mg) were dipped into 21.9, 2.5, 0.27, and 0.07 kBq tritium aqueous solutions in glass vials for about 3.5 min (until the tritiated water was sucked up from the bottom to the top of paper scintillator). The weight of absorbed water was 146.7 ± 0.6 mg. Tritium aqueous solutions were purchased from Japan Radioisotope Association (JRIA). Radioactivity was determined as follows: 0.1 mL of each tritium aqueous solution was added to a glass vial followed by the addition of 4 mL of LS (Ecoscint, National Diagnostics, Co. Ltd.). After each paper scintillator strip was immersed in a tritium aqueous solution, each wet strip was placed in a new glass vial. In both cases, the count rate was measured with a PerkinElmer 2100TR LSC for 3 min in ^3H mode by scintillation counting. After 71 min in the glass vials, the dry strips were placed into new glass vials and measured again.

Temporal Evolution of the Counting Efficiency of the Paper Scintillator. After an approximately 4 × 1 cm^2 strip of the paper scintillator (65.7 ± 2 mg) was dipped into a glass vial with 2.7 kBq tritiated water (137 Bq/mL) for 10 min, the paper was placed into a new glass vial with a cap to measure the count rate of tritium by scintillation counting for 3 min using a Hitachi LSC-7400. During the standing time, tritiated water evaporated from the paper and condensed on the glass wall (20 mL volume of typical glass vial for scintillation counting). Then, the paper was picked up and placed into a new glass vial. Subsequently, 8 mL of LS was poured into the glass vial contaminated with tritiated water and mixed. Radioactivity was determined by using the net count rate and the tritium counting efficiency of the LSC. The count rate of tritium of the new glass containing the paper was measured using LSC-7400. This procedure was repeated until the count rate of tritium of the paper became 0 cpm. Finally, the total tritium activity that remained in the paper scintillator was 23.1 Bq.

Similarly, after a 4 × 1 cm^2 strip of paper scintillator was dipped into water for 10 min in the glass vial, the wet paper was picked up and put into a new glass vial with a cap to measure their weights using an analytical balance (A&D Co. Ltd., HR-250AZ). The weight of absorbed water was 180.6 ± 0.4 mg. Each measurement was repeated three times to obtain the average value and standard deviation. During the standing time, water evaporated from the paper and condensed on the glass wall. Then, the paper was picked up and replaced into a new glass vial and the weight was measured. The weight of the evaporated water was calculated using the mass of an empty glass vial and the weight of the paper scintillator containing absorbed water.

RESULTS AND DISCUSSION

The paper scintillator was composed of scintillator−silica FPs and cellulose fibers, while the scintillator−silica FP was composed of silica NPs attached onto micrometer size silica FPs.[16,18,20] The silica NPs contain benzoic acid, PPO, and POPOP molecules. The scintillator−silica FP was pressed to form pellet, and the pellet showed luminescence peaked at 445 nm.[18] Luminescence was shifted from 410 nm that corresponds to the peak emission of cyclohexane from PPO and POPOP crystal scintillators.[21]

Photophysical Characterization of the Paper Scintillator. Figure 1 shows the excitation and emission spectra of the paper scintillator under ultraviolet excitation. Emission corresponded to a broad band from 330 to 600 nm that peaked at about 442 nm with a shoulder at about 460 nm. According to previous results, emission from PPO powder was observed within 350−500 nm and peaked at 389 nm under excitation at 365 nm, from POPOP powder within 400−600 nm and peaked at 468 nm under excitation at 405 and 425 nm, and from benzoic acid powder within about 250−600 nm and peaked at 310 nm under excitation at 280 nm.[18] According to those results, the emission band peaked at 442 nm with a shoulder at about 460 nm together with the emission at higher wavelengths was attributed to crystalline POPOP,[22] possibly including POPOP dimers,[23] and solvated POPOP.[24]

Further, under 302 nm excitation, photoluminescence within 350−400 nm was attributed to PPO and its relatively weak intensity due to partial absorption by POPOP. The lack of

https://doi.org/10.1021/acsomega.4c01901
ACS Omega XXXX, XXX, XXX−XXX

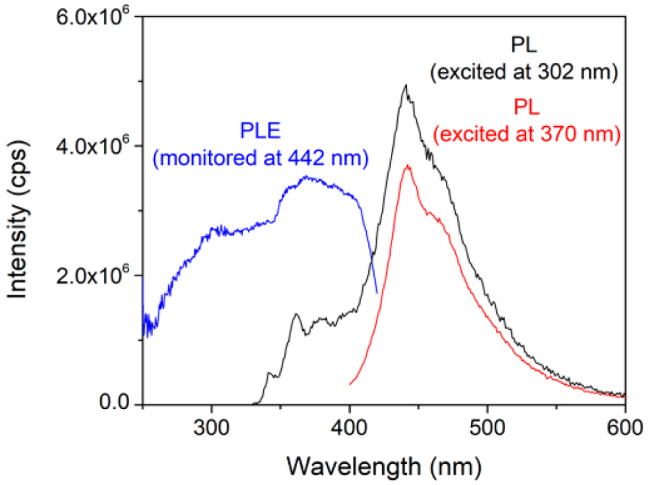

Figure 1. PLE spectrum monitored at 442 nm and emission (PL) spectra under ultraviolet excitation (302 and 370 nm) of our paper scintillator.

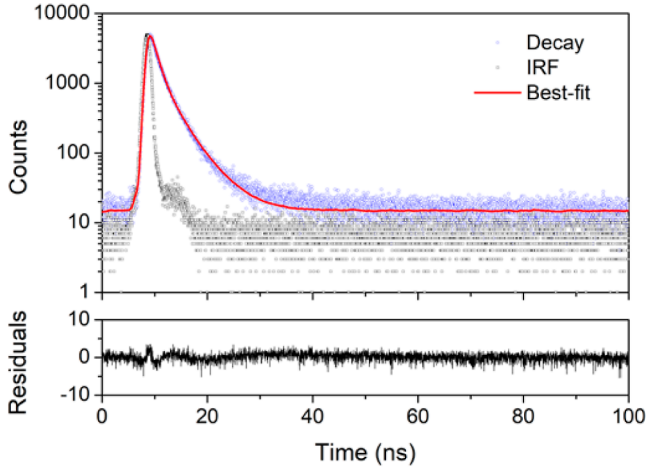

Figure 2. Photoluminescence decay of the paper scintillator measured at 442 nm under excitation at 362.8 nm.

intense photoluminescence within 300−350 nm showed that emission from benzoic acid was efficiently absorbed by POPOP and PPO. Under 370 nm excitation, which corresponds to the peak absorption of PPO, the emission spectrum had essentially the same shape as the one under 302 nm excitation above 400 nm. The lack of relatively intense emission near 400 nm showed that the PPO emission was efficiently absorbed by POPOP.

The excitation spectrum obtained monitoring at 442 nm, which corresponds to POPOP emission, yielded a continuum absorption spectrum wherein two overlapping broad bands at about 370 and 300 nm could be seen. The band at 370 nm was attributed to PPO and the band at 300 nm to benzoic acid. Moreover, the decreasing intensity for wavelengths below ∼300 nm was characteristic of the shape of the excitation band of POPOP, suggesting that the recorded excitation spectrum is a complex superposition of the excitation bands of all three organic compounds: POPOP, PPO, and benzoic acid. These results showed that POPOP efficiently absorbed the emissions from benzoic acid and PPO. Quantum efficiency was determined for excitations at 301 and 370 nm, as per photoluminescence excitation (PLE) results discussed above. At 301 nm, the average quantum efficiency from both faces of the paper scintillator was about 4%, and at 370 nm, it was about 11%.

Based on photoluminescence excitation results, the temporal decay of the main emission at 442 nm (blue open circles) was monitored under excitation at 362.8 nm, and the results are shown in Figure 2. Also shown are the IRF (black open squares), the result of the analysis with two exponential decays (red continuous line), and the residuals corresponding to the difference between the experimental decay results and the analysis result. Visual inspection showed the value of χ^2 = 1.3, where a low χ^2 value is an indication of good correlation between the fit and the experimental data, and the low value of the residuals confirmed the good quality of the analysis. The analysis yielded a 1.29 ± 0.01 ns main fast decay (64.2%) combined with a 4.00 ± 0.04 ns slower decay (35.8%). The main fast decay lifetime was attributed to solvated POPOP because its emission is peaked at 447 nm and because of its 1.7 ns lifetime.[24] On the other hand, the slow lifetime was attributed to the emission of crystalline POPOP, which has a reported peak emission at 471 nm and a lifetime of 2.34 ns,[24] excited by the emission of PPO that has a lifetime of 1.4 ns. The combined lifetime of 3.74 ns is very close to the obtained lifetime of 4.00 ns, and the difference was tentatively attributed to the absorption time. The above attributions suggested that most POPOP in the paper scintillator was solvated since the main emission is at 442 nm and 1.29 ns is the dominant (64.2%) lifetime. On the other hand, the relatively high contribution of 35.8% of the slow component indicated high efficiency of the absorption of PPO emission by POPOP.

The radioluminescence spectrum (black line; Figure 3) was composed by a main band with two peaks centered at 440 and

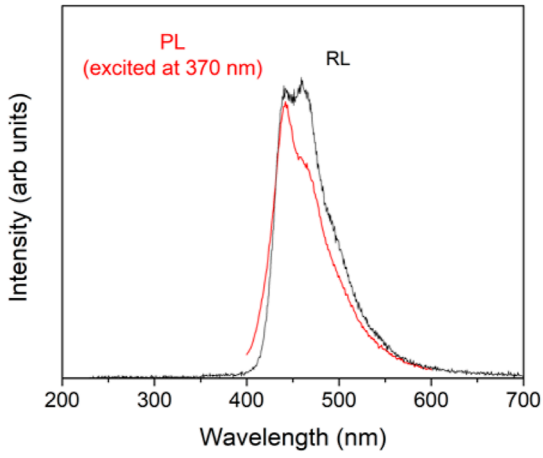

Figure 3. Radioluminescence spectrum (RL; black line) of the paper scintillator excited by X-rays and its photoluminescence spectrum (PL; red line) excited at 370 nm. The intensity of the spectra was adjusted to facilitate comparison.

460 nm and a long tail toward longer wavelengths, while no emission was observed below 400 nm. Also shown in Figure 3 is the photoluminescence spectrum obtained under excitation at 370 nm (red line). Besides a small difference in the relative intensity between the two peaks, both spectra were essentially the same. As per the discussion above, radioluminescence emission was attributed to crystalline and solvated POPOP. The lack of emission below 400 nm showed that all emissions

https://doi.org/10.1021/acsomega.4c01901
ACS Omega XXXX, XXX, XXX−XXX

from benzoic acid and PPO were effectively absorbed by POPOP.

Proof of Concept Demonstration of Tritium Detection. *Tritium Detection and Counting Efficiency of the Paper Scintillator.* Luminescence measurements described above confirmed that our paper scintillator contains organic scintillators such as PPO, POPOP, and benzoic acid molecules encapsulated in the silica NPs attached onto silica FPs (scintillator−silica FPs) within the cellulose fiber network. The absorption and emission spectra of the organic scintillators overlapped, and excitation of benzoic acid by β-particles is expected to continuously induce emission from POPOP. The hydrophilic nature of the paper scintillator allows for the absorption and retention of tritiated water in the pores of the cellulose fiber network and in the silica FPs, instead of just having a wet surface like with PS. Consequently, the silica FPs will retain tritiated water near scintillator−silica NPs throughout the whole volume of the paper. Usually, LS is composed of several organic solvents but can be mixed only with small quantities of tritiated water. Even with the use of a surfactant, the maximum mixture ratio with water is up to 54% (PerkinElmer Co. Ltd., Ultima Gold LLT).[25] On the other hand, since no organic solvents are needed, the paper scintillator can absorb larger volumes of tritiated water depending on the paper volume. Consequently, our paper scintillator is expected to detect tritium more effectively than PS. It is our goal to demonstrate the applicability of this novel scintillator material for the detection of β-particles, the advantage of the paper scintillator not requiring LS to work, and the generation of less waste.

The structure of the paper scintillator was characterized by SEM imaging, as shown in Figure 4a, where scintillator−silica FPs were found to be distributed among the cellulose fibers.

SEM imaging also showed considerable porosity capable of absorbing and retaining tritiated water. Fluorescence investigation under 365 nm LED excitation of both faces of the paper is shown in Figure 4b and d. Comparison of photographs obtained under 365 nm excitation shown in Figure 4b and d revealed one face of the paper (Figure 4d) to have considerably lower blue emission, indicating a lower number of scintillator−silica FPs. This is in agreement with the quantum efficiency results that revealed different efficiencies for each face of the paper scintillator. In Figure 4c, the luminescence spectra of each face obtained under 280 nm excitation are shown. The intense blue emission is missing in the spectrum that corresponds to Figure 4d (red spectrum). In fact, it is possible to consider this spectrum to be from the paper itself, essentially without the contribution of scintillator−silica FPs. This set of results demonstrates that luminescence comes from the scintillator−silica FPs but not from the cellulose fiber network.

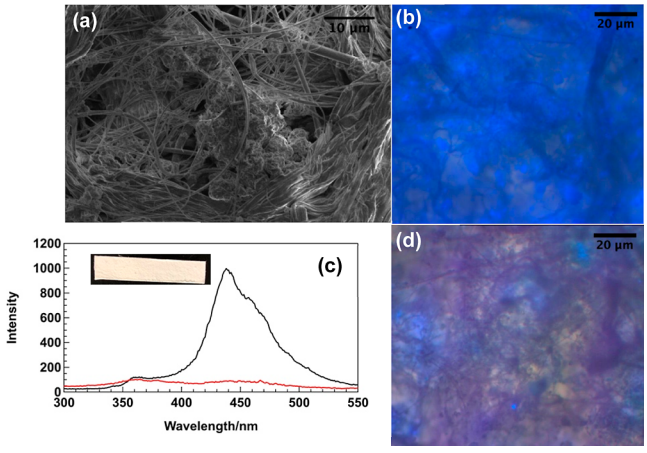

Figure 4. Typical images of the paper scintillator obtained by SEM (a) and under 365 nm LED light illumination (b). (a,b) are from different regions of the paper scintillator and with distinct scales. (c) Surface fluorescence spectrum of paper scintillator with excitation at 280 nm using a Shimadzu RF5300PC fluorometer (black line for (b); red line for (d)). Inset: photograph of the paper scintillator (area: 5.94 cm^2). (d) Image of the paper scintillator under 365 nm LED illumination showing less scintillator−silica FPs than in (b).

As illustrated in Figure 5a, the paper scintillator was dipped into tritiated water for about 3.5 min, until the tritiated water was absorbed all the way to the top of the paper scintillator, resulting in 146.7 ± 0.6 mg of tritiated water being absorbed into the paper scintillator.

This corresponds to a 145% increase in weight in relation to the dry paper scintillator. Figure 5b shows the net count rates of the wet paper scintillator after immersion in tritiated water solutions with various activities as well as after they dried for 71 min in closed glass vials. The net count rate of the dried paper scintillator was obtained after letting it dry for 71 min and placing it in a new glass vial. This time was not enough for all water to evaporate. As expected, the dried paper scintillator exhibited a lower count rate than when wet. This decrease was due to the evaporation of tritiated water from the paper onto the glass wall of the vials. On the other hand, in the case of plain paper without scintillator−silica FPs also dipped in tritiated water, no scintillation was detected. This demonstrates that the paper scintillator was able to detect β-particles from tritiated water absorbed in it.

It is noted that some of the tritiated water remained in the open spaces between the scintillator−silica FPs and the cellulose fibers such that the paper was not fully dried. Consequently, the net count rate of the dried paper increased with increasing activity of the tritiated water. Overall, the difference in net count rate between the wet and dried paper scintillator decreased from 200 to 36 dpm for higher activities of the tritiated solution. This is likely due to the fact that tritium at the surface of the scintillator−silica FPs is adsorbed and isotopically exchanged in the scintillator−silica FPs.

Figure 6 shows the counting efficiency of the dry paper scintillator against the activity of various tritiated water solutions. The counting efficiency was calculated by comparing the count rate (cpm) of the wet paper scintillator with the disintegration rate (dpm) of the absorbed volume. The volume of absorbed water was calculated from the mass of absorbed water (146.7 mg) and the density of water (1 g/cm^3) to be 0.147 mL. The calculated radioactivity of the absorbed tritiated water was about 96% of that of the tritiated solution released from the paper.

The radioactivity of the tritiated water was determined as follows: after 0.1 mL of the tritiated water was mixed with 8 mL of LS, they were set in the LSC to measure radioactivity using the counting efficiency of the LSC. The calculated radioactivity was obtained from the volume of tritiated water and the radioactivity of tritium.

$$\text{Counting efficiency of the paper scintillator (\%)} = \frac{\text{Net count rate (cpm)}}{\text{Calculated radioactivity of tritium (dpm)}} \times 100$$

https://doi.org/10.1021/acsomega.4c01901
ACS Omega XXXX, XXX, XXX−XXX

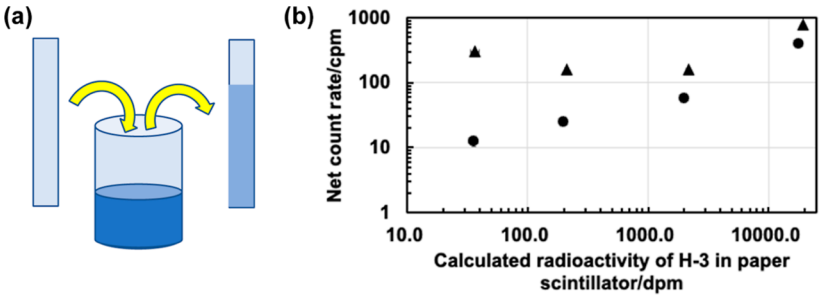

Figure 5. (a) Schematics of the dipping paper scintillator into tritiated water and the immediate water absorption. (b) Net count rate of the wet (triangle) and dried (circle) paper scintillator after immersion in tritiated water recorded by scintillation counting. The error bars are hidden within the respective symbols.

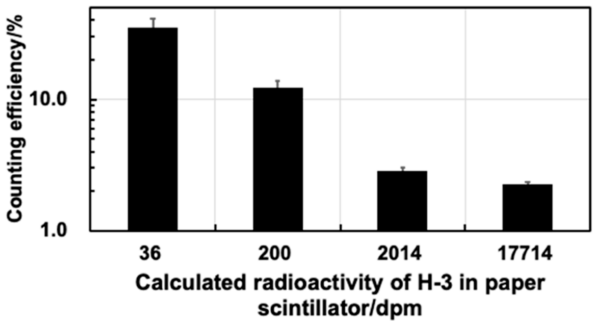

Figure 6. Counting efficiency of the paper scintillator against the calculated radioactivity of tritiated water. The calculated radioactivity was obtained from the volume of tritiated water and the radioactivity of tritium.

As shown in Figure 6, it was found that the apparent counting efficiency progressively increased for decreasing tritium concentrations, being above 30% for the 36 dpm tritiated water solution, indicating that the paper scintillator can work for tritium detection in water solutions more effectively without LS. That means that tritiated water close or in contact to the scintillator−silica FPs was preferentially evaporated. At lower radioactivity levels, less than 1000 dpm, the contribution of tritiated water at the interface of the scintillator−silica FPs is large, that is, tritium is likely adsorbed by the vapor pressure isotopic effect[26] and isotopically exchanged in the scintillator−silica FPs. Therefore, at lower radioactivity concentrations of tritium in water, β-particles from tritium can be effectively detected.

As the radioactivity of tritium remaining in the paper scintillator decreased, the counting efficiency increased. This phenomenon was also observed from a paper scintillator placed in glass vials as the tritiated water evaporated onto the glass vial wall. The glass vial was exchanged after each measurement of radioactivity. The counting efficiency was determined using the net count rate and tritium radioactivity remaining in the paper scintillator by placing the paper scintillator into a new glass vial.

As shown in Figure 7, overall, the counting efficiency increased with the decrease of radioactivity of tritium remaining in the paper scintillator. Since the vapor pressure of ^{3}H is lower than that of ^{1}H, $\left(\frac{P_{H_2O}}{P_{HTO}} = 1.10\right)$ at 20 °C,[27] it is easier for water to evaporate compared to tritiated water.[26] Due to the hydrophilic nature of the surface of the scintillator−silica FPs, it is likely that water remains within the space between the fibers (see Figure 1A). Eventually, the net count rate of the paper scintillator reached zero, indicating that all tritium was removed by evaporation. The total radioactivity of tritium was 23.1 Bq, corresponding to a volume of 0.168 mL based on 137 Bq/mL of tritium concentration.

Figure 8 shows the rate of evaporated water (circles) and tritium radioactivity (triangles) from a wet paper scintillator (data from Figure 7) against time in the glass vial at room temperature. Each rate of evaporated water was obtained by placing the wet paper scintillator in a new glass vial of known

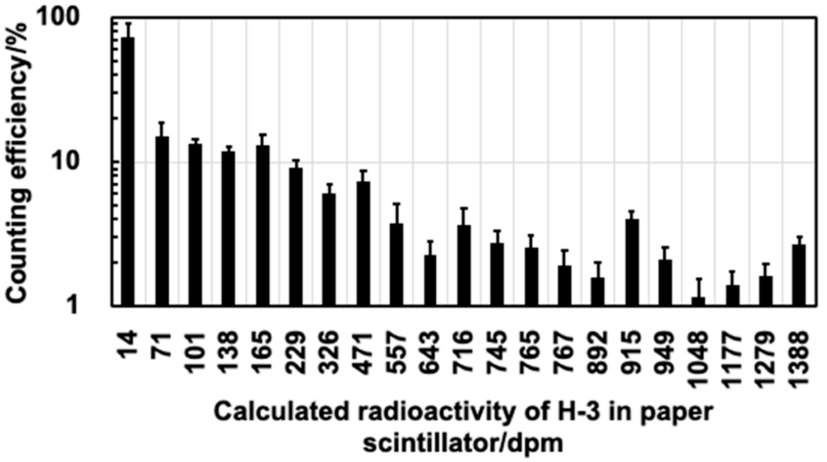

Figure 7. Plot of counting efficiency against radioactivity of tritium remaining in the paper scintillator placed in a glass vial.

https://doi.org/10.1021/acsomega.4c01901
ACS Omega XXXX, XXX, XXX−XXX

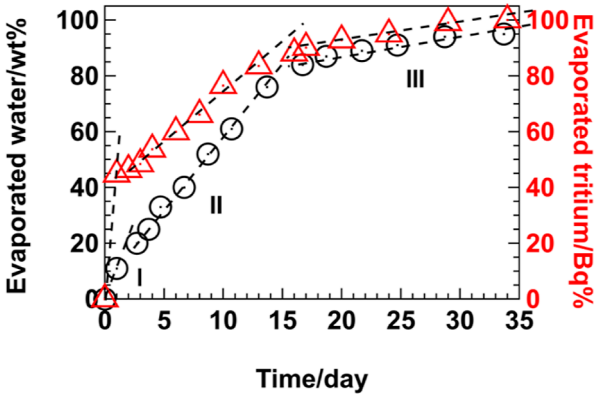

Figure 8. Plot of the rate of evaporated water (circles) and tritium radioactivity (triangles) from the wet paper scintillator against time in days. Each tritium radioactivity was extracted from the data in Figure 7. Each dashed line presents a slope of a linear approximation and is referred to as regions I, II, and III.

weight and measuring the weight of the glass vial with the wet paper scintillator. The difference in weight between a weight measurement and the previous weight measurement yielded the mass of evaporated water. In addition, each rate of evaporated tritium was also calculated using the radioactivity of tritium in Figure 7. After removing the paper scintillator, 8 mL of LS was poured into the empty glass vial, and the radioactivity was measured by scintillation counting. Radioactivity was due to tritium that evaporated from the wet paper scintillator onto the glass wall. Finally, once the paper scintillator had no net count rate, it meant that all tritium evaporated completely and the total tritium radioactivity was obtained by adding up each evaporated tritium radioactivity.

As shown in Figure 8, the evaporation rate of water has three different slopes: regions I, II, and III indicated by the dashed lines from 0 to 1, from 2.7 to 13.7, and from 16.7 to 33.7 days. These regions correspond to the slopes 11, 5.1 ± 0.1, and 0.64 ± 0.08(%/day), respectively. Also, the three regions correspond to the rate of evaporated tritium radioactivity: 44.7, 3.5 ± 0.1, and 0.66 ± 0.07 (%/day). The different slopes indicated that the evaporation of water in the paper, in the cellulose fiber network,[28] and absorbed water on the scintillator−silica FPs were different. The evaporation rate of the absorbed water is slower than that of water on and/or in the paper. It has been reported that the silica−water interface has two types of hydration, i.e., adsorbed molecular water and wet surface.[29] Regions I and II correspond to wet surface and III may correspond to adsorbed water because the slope of region III is much lower than that of regions I and II. Consequently, at lower radioactivity, tritium was preferentially adsorbed by the vapor pressure isotope effect[26,30] and isotopically exchange[26] on the surface of scintillator−silica FPs. The contribution of adsorbed tritiated water on the scintillator−silica FPs was larger than that at the inner or outer space of fibers. Because of the larger vapor pressure of water than that of tritiated water at 20 °C[27] and because the distance between tritium and scintillator−silica FPs was closer, the tritiated water remained on the silica FPs and on the scintillator-silica NPs. These conditions made it possible to more effectively detect the low energy (18.6 keV) and consequently short-range β-particles from tritium. Therefore, the counting efficiency of the paper scintillator increased at lower tritium radioactivity.

CONCLUSIONS

The paper scintillator was fabricated through the incorporation of scintillator−silica particles and investigated in its photophysical properties and response to tritium aqueous solutions with different activities. A complex exchange between benzoic acid, PPO, and POPOP was revealed by luminescence measurements. POPOP efficiently absorbed the emission from benzoic acid and PPO. Fluorescence decay at 442 nm excited at 362.8 nm had two components with the dominant short lifetime being due to solvated POPOP and the long lifetime to the PPO emission, its absorption, and re-emission by crystalline POPOP. Radioluminescence measurements confirmed the dominance of solvated POPOP over crystalline POPOP. Under excitation at 301 nm, quantum efficiency was determined to be about 4%, and at 370 nm, it was about 11%. LSC measurements of a paper scintillator indicated that low-energy β-particles from tritiated water could be effectively detected. Moreover, the counting efficiency of tritium increased above 10% for tritium activities lower than 200 Bq. The presence of significant porosity in the paper scintillator allowed for effective absorption and isotopic exchange of tritium on the surface of the scintillator−silica FPs. The presence of significant porosity in the paper scintillator allowed for more effective absorption of the tritiated water into the paper scintillator than that of PS. Further, the large surface area of the scintillator−silica FPs allowed for effective isotopic exchange between tritium and hydrogen by the vapor pressure isotope effect. Such combination created by the hydrophilic scintillator−silica FPs and the cellulose fiber network leads to higher sensitive detection of low-energy β-particles from tritiated water than from the current standard procedure using LS. In summary, these results demonstrated that our paper scintillator was effectively engineered to detect low-energy β-particles from tritium in aqueous solutions without LS.

AUTHOR INFORMATION

Corresponding Authors

Hirokazu Miyoshi − *Advance Radiation Research, Education, and Management Center, Tokushima University, Tokushima 770-8503, Japan*; orcid.org/0000-0003-0856-8410; Email: miyoshi.hirokazu@tokushima-u.ac.jp

Luiz G. Jacobsohn − *Department of Materials Science and Engineering, Clemson University, Clemson, South Carolina 29634, United States*; Email: luiz@g.clemson.edu

Authors

Mami Nakamura − *Advance Radiation Research, Education, and Management Center, Tokushima University, Tokushima 770-8503, Japan*

Elizabeth M. Tsekrekas − *Department of Materials Science and Engineering, Clemson University, Clemson, South Carolina 29634, United States*; orcid.org/0000-0001-9417-8827

Complete contact information is available at: https://pubs.acs.org/10.1021/acsomega.4c01901

Funding

This work was partially supported by Awa Paper Mfg., Co. Ltd., Tokushima, Japan from April 1st, 2018 to March 31st, 2019 (H. Miyoshi).

https://doi.org/10.1021/acsomega.4c01901
ACS Omega XXXX, XXX, XXX−XXX

Notes

The authors declare no competing financial interest.

■ ACKNOWLEDGMENTS

The authors thank Hiroura Co. Ltd. for providing the silica fine powders. The authors thank Ayumi Fukuhara of Awa Paper Mfg., Co. Ltd. for preparing the scintillation paper. This material is partially based upon work supported by the National Science Foundation under Grant no. DMR-1653016 (L.G. Jacobsohn, E.M. Tsekrekas) and JST A-STEP JPMJTM20RP (H.M., M.N.). The authors thank Tomoyuki Ueki of the Institute of Technology and Science Center of Tokushima University for technical support in SEM imaging of the paper scintillator.

■ REFERENCES

(1) L'Annunziata, M. F. *Handbook of radioactivity analysis*; Academic Press, Elsevier, 2020; Vol. *1*.
(2) Kang, H.; Min, S.; Seo, B.; Roh, C.; Hong, S.; Cheong, J. H. Low energy beta emitter measurement: a review. *Chemosens* **2020**, *8*, 106.
(3) Bricks, J. B. *The theory and practice of scintillation counting*; Pergamon Press: Oxford, 1964.
(4) IAEA. *Safety Reports Series No. 67, Monitoring for compliance with exemption and clearance levels*; IAEA: Vienna, 2012.
(5) Furuta, E.; Ohyama, R.; Yokota, S.; Nakajo, T.; Yamada, Y.; Watanabe, Y. The effect of atmospheric plasma treatments on plastic scintillator for beta-ray measurement. *J. Radioanal. Nucl. Chem.* **2014**, *299*, 471−476.
(6) Furuta, E.; Kawano, T. A plastic scintillation counter prototype. *Appl. Radiat. Isot.* **2015**, *104*, 175−180.
(7) Yoshihara, Y.; Furuta, E.; Ohyama, R.; Yokota, S.; Kato, Y.; Yoshimura, T.; Ogiwara, K. Measurement of tritium with plastic scintillator surface improvement with plasma treatment. *Fusion Sci. Technol.* **2015**, *67* (3), 654−657.
(8) Furuta, E.; Kato, Y.; Fujisawa, S. Measurement of tritium with plastic scintillators in large vials of a low background liquid scintillation counter: an organic waste-less method. *J. Radioanal. Nucl. Chem.* **2017**, *314*, 701−708.
(9) Morishita, Y.; Hoshi, K.; Torii, T. Evaluation of an ultra-thin plastic scintillator to detect alpha and beta particle contamination. *Nucl. Instrum. Methods Phys. Res., Sect. A* **2020**, *966*, 163795.
(10) Koshimizu, M.; Yanagida, T.; Kamishima, R.; Fujimoto, Y.; Asai, K. Scintillation properties and α-ray detection capabilities of thin-film plastic scintillators. *Sens. Mater.* **2019**, *31* (4), 1233−1239.
(11) Gledhill, J. A. The range-energy relation for 0.1-600 keV electrons. *J. Phys. A: Math., Nucl. Gen.* **1973**, *6* (9), 1420−1428.
(12) Jacobsohn, L. G.; Bennett, B. L.; Muenchausen, R. E.; Smith, J. F.; Wayne Cooke, D. Luminescent properties of nanophosphors. *Radiat. Meas.* **2007**, *42*, 675−678.
(13) McKigney, E. A.; Del Sesto, R. E.; Jacobsohn, L. G.; Santi, P. A.; Muenchausen, R. E.; Ott, K. C.; Mark McCleskey, T.; Bennett, B. L.; Smith, J. F.; Wayne Cooke, D. Nanocomposite scintillators for radiation detection and nuclear spectroscopy. *Nucl. Instrum. Methods Phys. Res., Sect. A* **2007**, *579*, 15−18.
(14) Jacobsohn, L. G.; Sprinkle, K. B.; Kucera, C. J.; James, T. L.; Roberts, S. A.; Qian, H.; Yukihara, E. G.; DeVol, T. A.; Ballato, J. Synthesis, luminescence and scintillation of rare earth doped lanthanum fluoride nanoparticles. *Opt. Mater.* **2010**, *33*, 136−140.
(15) Miyoshi, H.; Ikeda, T. Preparation of paper scintillator for detecting ^{3}H contaminant. *Radiat. Prot. Dosim.* **2013**, *156* (3), 277−282.
(16) Miyoshi, H.; Hiroura, M.; Tsujimoto, K.; Irikura, N.; Otani, T.; Shinohara, Y. Preparation of new scintillation imaging material composed of scintillator−silica fine powders and its imaging of tritium. *Radiat. Proc. Dosim.* **2017**, *174* (4), 478−484.
(17) Janczak, C. M.; Calderon, I. A. C.; Mokhtari, Z.; Aspinwall, C. A. Polystyrene-core, silica-shell scintillant nanoparticles for low-energy radionuclide quantification in aqueous media. *ACS Appl. Mater. Interfaces* **2018**, *10*, 4953−4960.
(18) Miyoshi, H.; Gotoh, H.; Hiroura, M.; Yamanaka, Y.; Irikura, N.; Otani, T.; Yamamoto, Y. Enhancement of counting efficiency for tritium using light-excited scintillator−silica pellets. *J. Radioanal. Nucl. Chem.* **2017**, *311* (3), 1991−1999.
(19) Etale, A.; Onyianta, A. J.; Turner, S. R.; Eichhorn, S. J. Cellulose: a review of water interactions, applications in composites, and water treatment. *Chem. Rev.* **2023**, *123*, 2016−2048.
(20) Miyoshi, H.; Nakamura, M. Preparation of paper scintillators and their effective use in radiation testing for α- and β- particles in radioactive liquid, solid, and gas contaminants. *Appl. Radiat. Isot.* **2024**, *206*, 111240.
(21) Yang, W.; Lee, E. K. C. Liquid scintillation counting: Singlet-singlet energy transfer processes. *J. Chem. Educ.* **1969**, *46* (5), 277−281.
(22) Lakowicz, J. R. *Principles of Fluorescence Spectroscopy*, 3rd ed.; Springer: New York, 2010; p 883.
(23) Dutta, A. K. Spectroscopic study of nonamphiphilic 2,2'-p-phenylenebis(5-phenyloxazol)(POPOP) assembled in supramolecular Langmuir-Blodgett films. *J. Phys. Chem. B* **1997**, *101*, 569−575.
(24) Yan, D.; Fan, G.; Guan, Y.; Meng, Q.; Li, C.; Wang, J. Tuning solid-state blue and red luminescence by the formation of solvate crystals. *Phys. Chem. Chem. Phys.* **2013**, *15*, 19845−19852.
(25) Parker, A. J.; Aspinall, M. D.; Boxall, C.; Cave, F. D.; Joyce, M. J. Radiometric techniques for the detection and assessment of tritium in aqueous media - a review. *Prog. Nucl. Energy* **2023**, *162*, 104733.
(26) Rosson, R.; Jakiel, R.; Kahn, B. Isotopic exchange and vapor pressure isotope effect in tritium oxide adsorption on silica gel. *J. Phys. Chem. B* **1998**, *102*, 10342−10346.
(27) Baumg artner, F.; Kim, M.-A. Isotope effects in the equilibrium and non-equilibrium vaporization of tritiated water and ice. *Appl. Radiat. Isot.* **1990**, *41* (4), 395−399.
(28) Zou, Y.; Maillet, B.; Brochard, L.; Coussot, P. Fast transport diffusion of bound water in cellulose fiber network. *Cellulose* **2023**, *30*, 7463−7478.
(29) Papirer, E. *Surfactant Science Series Volume 90, Adsorption on Silica Surfaces*; Marcel Dekker: New York, 2000; p 279.
(30) Kalinichenko, E. A.; Pushkarova, R. A.; Fenoll Hach-Alí, P.; López-Galindo, A. Tritium accumulation in structures of clay minerals. *Clay Miner.* **2002**, *37*, 497−508.

https://doi.org/10.1021/acsomega.4c01901
ACS Omega XXXX, XXX, XXX−XXX